

High-resolution Multi-reflection Time-of-Flight Mass Spectrometer with Atmospheric Pressure Interface

Zhengxu Huang¹, Shuxiong Yan¹, Yi Ren¹, Qi Huang¹, Yi Hong², Zhengge Chen¹, and Mei Li¹

¹Jinan University

²Guangzhou Hexin Instrument Co Ltd

July 20, 2023

Abstract

RATIONALE: Many chemical processes operate at unsteady state and require a rapid mass analysis of transients with high resolution. An atmospheric pressure interface multi-reflection time-of-flight mass spectrometer (API-MRTOF-MS) has the potential to be a powerful process analytical tool. **METHODS:** The ion flight path of the API-MRTOF-MS was extended from meters to over one kilometer, and the mass resolution was increased to an ultra-high level. Furthermore, the mass analysis could be done at around ten milliseconds due to the rapidity of TOFMS. The mass analyzer reflects ions via electrostatic mirrors and directs them along a folded flight path, significantly increasing flight distances and theoretically with no upper limit. The powerful API, equipped with two quadrupoles, makes the API-MRTOF-MS suitable for complex mass spectrometry methods with alternative ion selection schemes. **RESULTS:** A mass resolution of 116,050 for Cs⁺ ions is achieved within a total time-of-flight of only 18 ms. An ion transmission efficiency of over 50% was achieved after 600 cycles. **CONCLUSIONS:** The performance of the API-MRTOF-MS demonstrates that it is exceedingly suitable for high-resolution process analysis, particularly for transient process analysis, due to its fast analysis speed and high-selectivity.

High-resolution Multi-reflection Time-of-Flight Mass Spectrometer with Atmospheric Pressure Interface

Shuxiong Yan^{1,2}, Yi Ren^{1,3*}, Qi Huang^{1,4}, Yi Hong³, Zhengge Chen^{1,4}, Mei Li¹, Zhengxu Huang^{1,3**}

1(Institute of Mass Spectrometry and Atmospheric Environment, Jinan University, Guangzhou, 510632, China)

2(Shenzhen Institute of Advanced Technology, Chinese Academy of Sciences, Shenzhen, 518055, China)

3(Guangzhou Hexin Instrument Co., Ltd. Guangzhou, 510530, China)

4(Guangdong MS Institute of Scientific Instrument Innovation, Guangzhou, 510000, China)

E-mail addresses: *y.ren2@hxmass.com* (Y.Ren*), *hzx126@126.com* (Z.Huang**)

Abstract:

RATIONALE : Many chemical processes operate at unsteady state and require a rapid mass analysis of transients with high resolution. An atmospheric pressure interface multi-reflection time-of-flight mass spectrometer (API-MRTOF-MS) has the potential to be a powerful process analytical tool.

METHODS : The ion flight path of the API-MRTOF-MS was extended from meters to over one kilometer, and the mass resolution was increased to an ultra-high level. Furthermore, the mass analysis could be done at around ten milliseconds due to the rapidity of TOFMS. The mass analyzer reflects ions via electrostatic mirrors and directs them along a folded flight path, significantly increasing flight distances and theoretically

with no upper limit. The powerful API, equipped with two quadrupoles, makes the API-MRTOF-MS suitable for complex mass spectrometry methods with alternative ion selection schemes.

RESULTS : A mass resolution of 116,050 for Cs⁺ ions is achieved within a total time-of-flight of only 18 ms. An ion transmission efficiency of over 50% was achieved after 600 cycles.

CONCLUSIONS : The performance of the API-MRTOF-MS demonstrates that it is exceedingly suitable for high-resolution process analysis, particularly for transient process analysis, due to its fast analysis speed and high-selectivity.

Keywords : Multi-reflection time-of-flight mass spectrometer, atmospheric pressure interface, high-resolution, rapid mass analysis, process analytical technology

Introduction

With continuous improvement over the past 30 years, multi-reflection time-of-flight mass spectrometer^{1, 2} (MRTOF-MS) was established as a potent analysis tool in physics³⁻¹⁴ for its ability to perform high-resolution and fast mass analysis. These properties are also essential for analysis in chemistry, biology, and medicine¹⁵⁻²⁰. Meanwhile, process analysis has become an emerging discipline in analytical sciences that poses special requirements on analytical techniques²¹⁻²⁵, particularly in the context of transient process analysis²⁶. This type of process analysis requires high analyzing speed. The MRTOF-MS may couple with various ionizations and meet all requirements through an atmospheric pressure interface (API), which makes it an effective process analytical instrument.

Several groups have attempted to couple atmospheric ionization²⁷⁻²⁹ with the MRTOF-MS for various applications. T. Dickel et al.^{30, 31} developed a compact MRTOF-MS for in-situ applications by directly connecting a simple API to the apparatus. S. Naimi et al.³² coupled electrospray ionization (ESI) with MRTOF-MS using an ion carpet device to offer a reference ion for nuclear mass measurements. Other studies that share a similar geometry with the MRTOF analyzer as a linear electrostatic ion trap^{33, 34} also presented various designs^{35, 36} with API. While these types of instruments have not been developed up until now. A. Verentchikov et al.^{37, 38} introduced a planar MRTOF technique, and the company Waters launched its new product, MRT³⁹, which utilizes this planar MRTOF technique and has a resolving power of 200,000. Thermo Scientific also introduced a high-resolution product called Orbitrap Astral⁴⁰, containing a similar planar MRTOF with a resolving power of 80,000. Planar MRTOF has a wider mass range than an axial MRTOF, but it requires more control over the energy distribution in the perpendicular direction. This energy distribution sets limits on the flight length and resolution.

In this study, we introduce an atmospheric pressure interface multi-reflection time-of-flight mass spectrometer (API-MRTOF-MS) that can do the high-resolution and rapid mass spectrometry with alternative ion selection schemes. The analyzer design is based on the ZD-MRTOF-MS^{41, 42} from KEK (Japan) at the SLOWRI facility⁴³, which achieves unprecedented mass resolving powers, i.e., $R_{FWHM} = m / \Delta m = t / 2\Delta t > 1 \times 10^6$, where m and t are the ion's mass and time of flight, whereas Δm and Δt are the full widths at half maximum (FWHM) of the mass and TOF spectral peaks, respectively. A set of ion transmission devices is specially designed for coupling with atmospheric ionizations, which could improve the duty cycle and supply a variety of ion selection capabilities. A differential pumping system that covers a massive pressure difference of 10 orders of magnitude is introduced. Test results of performance of the instrument are presented.

Apparatus

2.1 Apparatus structure

Our API-MRTOF-MS for molecular analysis consists of two subsystems. The API subsystem, modified from our API-TOF^{44, 45}, is designed for high-efficiency transport of ions from atmospheric ion sources. The API is composed of a heated stainless-steel capillary to separate atmospheric pressure and reduce depositions, a small radio-frequency-only quadrupole (RFQ) labeled MIR^{46, 47} in Fig. 1, and two larger quadrupoles serve as RFQs⁴⁸ (RFQ1 and RFQ2) to cool and transport the ions, providing efficient ion transport with the

capability of mass selection to improve the sensitivity for low-abundance materials. RFQ1 is designed with the ability to bunch ions, as introduced in Ref.⁴⁹. Through cooperating with the following ion trap, bunch mode could theoretically improve the duty cycle to 100% and supply an alternative ion selection scheme. RFQ2 serves as a quadrupole mass filter and can assist MS/MS experiments. Moreover, the API offered great flexibility in the choice of the ion source.

The following MRTOF subsystem consists of a flat ion trap (FLT)⁵⁰, an accelerating einzel lens (AC), a double steerer unit (ST), a set of drift tubes (DT), and the MRTOF analyzer. In the symmetric coaxial MRTOF analyzer, the mirror electrodes are aligned coaxially by eight independent gridless ring-mounted electrodes. Low-pass RC filters are applied to improve the stabilization of the voltages at the mirror endcap electrodes (1 M Ω , 4–8 μ F). The axisymmetric electrostatic field made by MRTOF analyzer is presented in Fig. 1. MRTOF-MS uses the concept of recycling the path length in a time-of-flight analyzer for multiple reflections⁵¹. The components of the MRTOF analyzer are described in great detail in Refs.^{42, 52}. Unlike the design in these references, we designed a shorter DT and moved the MRTOF analyzer closer to the FLT. This helps to expand the mass range of ions injected into the analyzer, but it will increase the gas load in the analyzer. The symmetric coaxial mirror electrode arrangement gives the analyzer more potential for higher resolution.

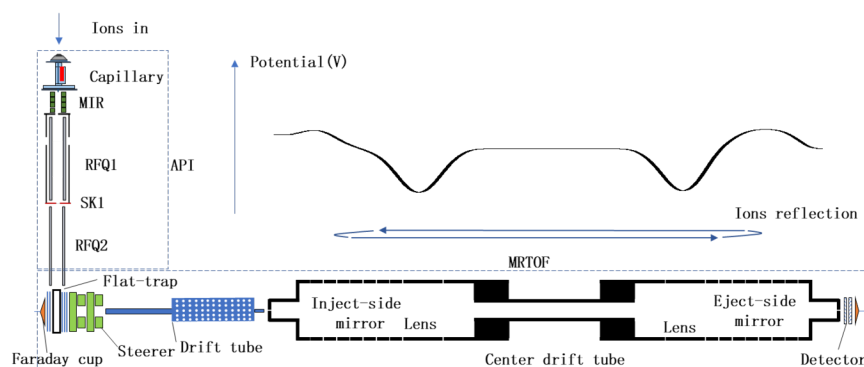


Fig. 1. Schematic overview of the API-MRTOF-MS and electric potential distribution (insets) along the axis of the MRTOF analyzer. From top left to bottom right, elements encompass the API subsystem and the MRTOF subsystem, outlined by dotted boxes. Ions are confined axially between the two ion mirrors as long as their kinetic energy is lower than the maximum potential in the mirrors.

2.2 Time pattern

The typical measurement cycle is as follows: First, ions are generated by atmospheric pressure ionization and introduced into the instrument through the capillary inlet. In the API region, the diameter of the ion beams can be reduced to the submillimeter range by collision action in the RFQs. Then, the ions are transferred to the FLT and trapped by the voltage of the endcaps switched up. After a final cooling in the FLT, the ions are ejected orthogonally, accelerated by the AC, and ion-optically adjusted by the ST and DT. Finally, the ions enter the MRTOF analyzer and reflect back and forth, increasing the ion flight distance from meters to hundreds of meters or even kilometers. After a predetermined number of reflections, the ejection endcap switches down and allows the ions travel to a micro-channel plate ion detector (MCP, R3809U, Hamamatsu). The timings for the FLT ejection and both mirror endcaps switching are mass dependent (as shown in Fig. 2), thus requiring a precalculated timing pattern.

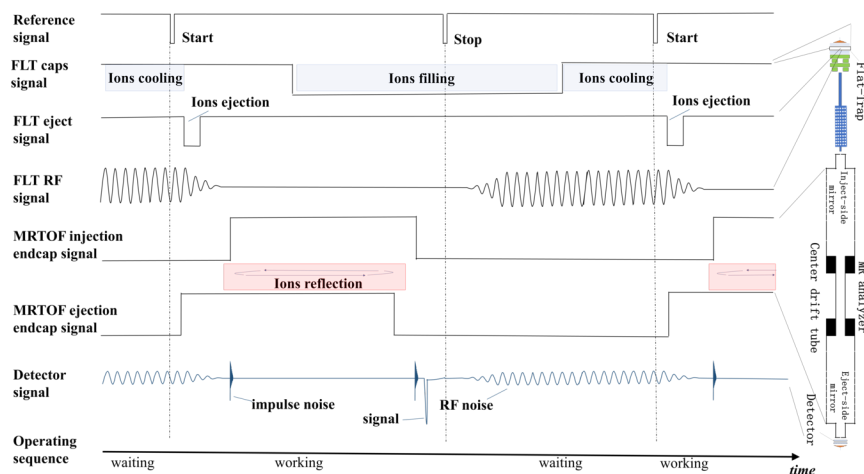


Fig. 2. Event sequence of experimental cycles. The vertical dashed lines symbolize (from left to right) the start signal, the end signal and the start signal of the next cycle.

Furthermore, by utilizing the RFQs and FLT, the API-MRTOF-MS can operate in bunch mode, resulting in higher duty cycle and enabling ion selection. In the typical continuous mode shown in Fig. 2 (FLT caps signal), ions are only utilized during ion filling time, and the duty cycle is determined by the ratio of filling time to cycle time. While in the bunch mode shown in Fig. 3, ions can be preserved by RFQ1, allowing for a 100% duty cycle. Moreover, by adjusting the pulse time of the FLT end cap, the instrument can choose ions based on their mass-to-charge ratio. Selectivity is vital for the analysis of processes, which often presents unique demands on analytical techniques, especially when dealing with complex samples. The high-resolution and fast mass analysis provided by API-MRTOF-MS will enable the analysis of transient processes. There are two ways that aid in progress: releasing unwanted small ions and preventing unwanted large ions from entering. Also, RFQ2 could act as a quadrupole for coarse ion selection. This section also addresses the issue of mass bandwidth improvement, which will be reported elsewhere in the near future.

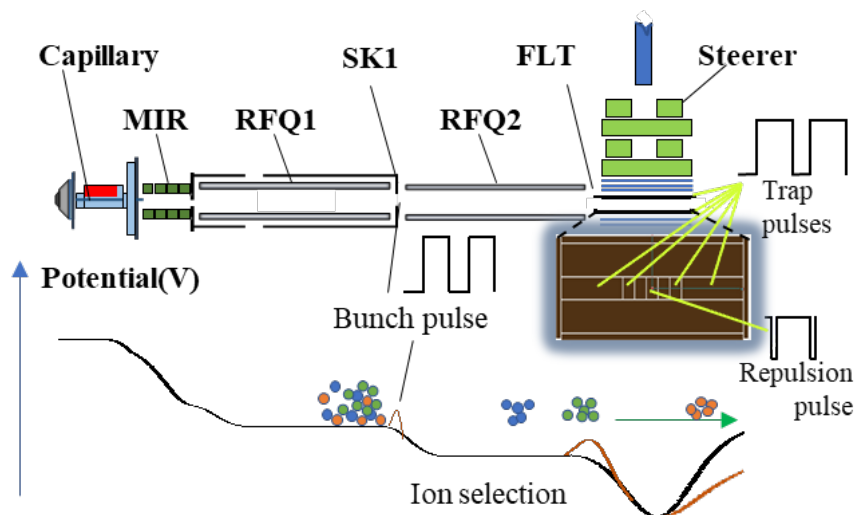


Fig. 3. Illustration of the bunch mode and ion selection scheme.

2.3 Vacuum system

As stated above, the ion flight distance shall be extended, which in turn requires a long mean free path length of the ions.

$$\lambda = \frac{kT}{\sqrt{2}\sigma p},$$

with the gas pressure p , the collision cross-section σ , the temperature T , and the Boltzmann's constant k . Here, the mean free path is inversely proportional to pressure ($\lambda \propto 1/p$); thus, the analyzer chamber must be maintained in an ultra-high vacuum to reduce the collision rate and prolong the ion flight length.

Compared with the ZD-MRTOF-MS at SLOWRI, the vacuum system of the API-MRTOF-MS became more complex. A large acceptance is required to achieve high transmission efficiency with the continuous sampling from atmospheric ionizations. Considering the high vacuum analyzer chamber, the differential vacuum system that covers a massive pressure difference is precisely designed using gas-flow calculations.

The Knudsen number (K_n) and the Reynolds number (R_e) are calculated to characterize the type of gas flow (see Ref. ⁵³page 14). Then, the conductance of a orifice and a long pipe in laminar flow and molecular flow are well described by simple formulas in Ref.⁵³.

In a balanced system, the gas flow Q is then given by

$$Q = (-) \times C = \times S,$$

which is proportional to the pressure difference of neighboring domains $(-)$, with the flow conductance C , and is equal to the product of the pressure of next stage vacuum P_1 and the pumping speed of a vacuum pump S .

We translate the theoretical concepts, calculations, and requirements into a dedicated design. As a prototype, we prefer to use the previous components and chambers. The vacuum system for the API-MRTOF-MS includes four metal chambers, as shown in Fig. 4. These chambers are custom made of cast aluminum alloy and sealed by "O-ring" seals (Fluoroelastomer). This design is solely for the prototype and not a true ultra-high vacuum system, but it still achieves the required vacuum level. Our miniature MRTOF-MS will make use of the improved vacuum design.

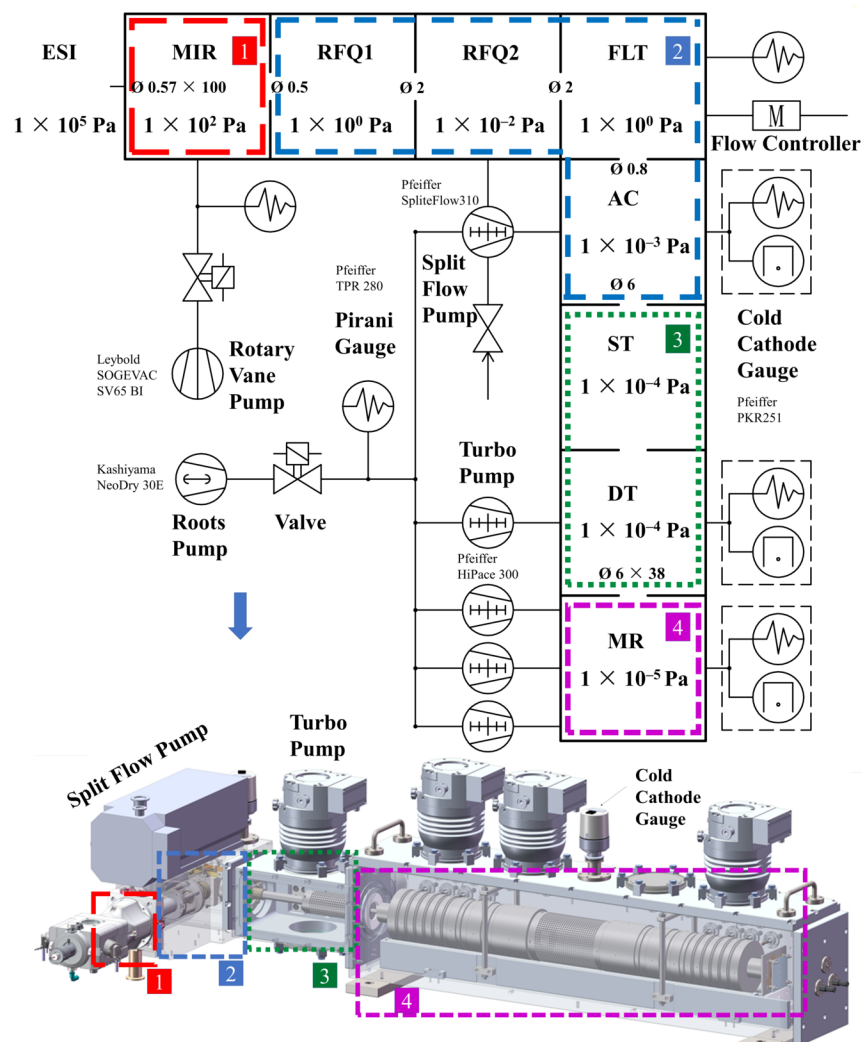


Fig. 4. Sketch of the vacuum system (upper) and its corresponding position in a schematic of API-MRTOF-MS (lower); the dotted and dashed rectangular frames with different colors indicate the four main chambers of the instrument: (1) MIR chamber, (2) RFQs and FLT chambers, (3) ST and DT chambers, (4) MRTOF analyzer chamber. Differential pumping stages and pressure in each compartment are present. The aperture diameters are presented in mm.

The API-MRTOF-MS apparatus is in the shape of the letter “L” with a length of 2230 mm, coupled with ESI ionization on the left. Each chamber contains electrical feedthroughs, most of which are multi-feedthroughs, except those for the ultrahigh voltage supplies. Heating plaster containing the silicone heating sheet inside is utilized to cover both sides of the MRTOF analyzer chamber, which can maintain a maximum chamber temperature of 80 to obtain a better vacuum. Table 1 lists the pressure of each chamber marked in Fig. 4, along with the pumping speed of the used pump. All turbo pumps are backed up by a 6 L/s roots pump (NeoDry 30E, Kashiyama).

Table 1 Chamber pressure with and without load

No.	Chamber Label	Pumping Speed (L/s)	Pump model	No Load Pressure (Pa)	Normal Load
1	MIR	18	SOGEVAC SV65 BI FC, Leybold	135	135

No.	Chamber Label	Pumping Speed (L/s)	Pump model	No Load Pressure (Pa)	Normal Load
2	RFQ1	/	/	/	/
3	RFQ2	250	SpliteFlow310, Pfeiffer	/	/
4	FLT	/	/	0.22	6.93
5	AC	200	SpliteFlow310, Pfeiffer	1×10^{-4}	1.55×10^{-3}
6	ST&DT	300	HiPace 300, Pfeiffer	1.52×10^{-5}	4.76×10^{-5}
7	MR	300*3	HiPace 300, Pfeiffer	8.57×10^{-6}	8.47×10^{-6}

Experiment setting

3.1

Ionization Source

The ESI operating voltage was 3800 V, the gas pressure was 0.4 MPa (N_2 standard gas with purity [?] 99.999%, Guangzhou Yuejia Gas), and the inlet temperature was 180 degC. With the strong electric field between the liquid and the inlet capillary of the interface, a so-called Taylor cone was formed. The instable charged droplets evaporated from the tip of the cone and drift to the inlet. Coulomb fission of the droplet happened as its radius approaches the Rayleigh limit⁵⁴, resulting in gas-phase ions. The heated inlet capillary efficiently improved the ionization process and kept neutral gas away.

3.2 Sample Preparation and Data Acquisition

Cesium ions with a nominal average molecular weight of 133 Da were used to test the characteristics of the API-MRTOF-MS. Solutions were prepared in acetonitrile at different concentrations (CsI, Sigma-Aldrich) and infused at a flow rate of $5 \mu\text{L min}^{-1}$ using a syringe pump (Harvard Pump 11 Elite, Harvard).

Ion signals were acquired with an oscilloscope (500 MHz, Keysight DSOX3052A, Keysight) with 2 ns resolution and subsequently transferred to a computer for display analysis.

3.3 MS measurement pattern

As described in Section 2, at this stage in the experiment, the API subsystem works in a continuous transport pattern; all three quadrupoles are RFQs that work as ion coolers, cooling ions by collision with residual gases without selection or bunch function, bunch function is not enable. The ions are cooled by collision with lighter buffer gases for extra 5 ms at a pressure of ~ 7 Pa. The transfer section following the FT is similar to that in Ref.⁴² but without the pulsed drift tube. The measurement cycle is triggered by a free-running timing system.

Results and discussion

4.1 Testing of the vacuum system

The vacuum system is redesigned to offer an ability to couple with atmospheric ionizations while preserving the ultra-high vacuum inside the MRTOF chamber. We recorded the pressure change in the analyzer using a cold cathode gauge (PKR251, Pfeiffer) with respect to the pumping time at a heating temperature of 100 , which corresponds to about 60 on the chamber.

The pumping process depicted in Fig. 5 is described by an exponential reduction in pressure, with a slower decreasing trend after the pumping period exceeds 9 hours. For metal vacuum chambers, the desorption of water vapor and adsorbed gases and the outgassing from seals lengthen the pump-down time⁵³. The process can be shortened by baking out the chambers. After long-time baking, the best pressure in the analyzer reached up to 6.8×10^{-6} Pa for our API-MRTOF-MS, corresponding to a mean free path of 2 km. The result indicates that a baking time of several days is necessary to achieve high vacuum.

Fig. 5. Experimental results of pressure in analyzer as a function of pumping time.

As we reduced the length of the DT between the FLT and the MRTOF analyzer in the design, the analyzer pressure changes must be tested with different cooling gas pressures. We regulated the pressure in the FLT by manually adjusting the intake gas valve. The pressure variation was recorded and compared with the results calculated by the method mentioned in Section 3.

As illustrated in Fig. 6, the FLT outer chamber pressure (Fig. 6A) and the DT chamber pressure (Fig. 6B) increase with the buffer gas pressure, showing a similar tendency with the calculation results. While the experimental results do not change much in comparison with the calculation results, according to the different scales of y-axes, the calculated pressures are about five to six times higher than those in the experiment. In contrast in Fig. 6C, the experimental data differs from the calculated trend. The buffer gas injection process appears to have no effect on the analyzer pressure which is mainly due to the elastomer sealing components (“O-ring”) we used. The diffusion through elastomer seals and their desorption rates caused limitations of the vacuum. These considerations will be used in future vacuum chamber designs to realize an improved vacuum. The differential vacuum system was carefully arranged with a pressure of 6.8×10^{-6} Pa.

Fig. 6. Measured pressures for different buffer-gas pressures in the FLT. Comparison of calculation and experimental results of the pressure outside the FLT (A), the pressure in the drift tube chamber (B), and the pressure in the MRTOF analyzer (C).

4.2 Performance of the API-MRTOF-MS

4.2.1 Signal intensity varying with lap numbers

Signal degradation over a long flight time is inevitable due to collisions of ions with the residual gas inside the analyzer, which is crucial for multicycle flight. About 10 ppm methanol solution of CsI was used to investigate the characteristics of signal variation with increasing flight distance. The ESI worked in a positive mode.

Fig. 7 shows the measured intensity at different laps. The signal is not stable for the first few laps, which can be attributed to the part of the ions not matching the phase-space acceptance of the analyzer (see also the corresponding response for the TOF distribution Δt in Fig. 9). Then, the signal suffers from a monotonic slow decay with increasing flight length. For the current situation, the transmission of the ions over 600 revolutions is about 50%, with a course of the order of 1.2 km.

Fig. 7. Signal intensity of $^{133}\text{Cs}^+$ ions as a function of the number of laps performed in the API-MRTOF-MS. At the highest lap number 667, the ions’ flight length is 1.2 km, and the corresponding time-of-flight is 20 ms.

4.2.2 Detection limit

Compared with other MRTOF-MS in nuclear physics, API-MRTOF-MS suffers from extra background, such as the chemical noise from sample injection from the atmosphere, and the electromagnetic interference from the ambient environment leaving noise to the spectrum⁵⁵. Thus, the detection limit is another crucial parameter. Taking CsI as the sample, we diluted the sample into concentrations of 1 ppm and 100, 10 and 1 ppb. Using the ESI to ionize the samples, we conducted a series of experimental tests. A signal-to-noise ratio (S/N) [?] 3:1 was accepted as the detection limit.

Fig. 8 shows the spectrum of $^{133}\text{Cs}^+$ recorded directly with the oscilloscope at a concentration of 10 ppb. The intensity of the $^{133}\text{Cs}^+$ peak is 9.84×10^{-2} mV, the calculated standard deviation of the noise is 1.23×10^{-2} mV, and the S/N is 8. Thus, we obtain a detection limit of 10 ppb, which is a meaningful value in a situation where a flight distance of more than 1 km is implemented. In this detection level, API-MRTOF-MS can be used in many scientific fields.

Fig. 8. Spectrum of $^{133}\text{Cs}^+$ at a concentration of 10 ppb.

4.2.3 Mass Resolving Power

After a series of optimizations that enabled a hundredfold-magnified flight length, experiments on measuring mass resolving power with CsI were performed. First, we investigated the mass resolution as a function of

the lap number. Then, we carefully tuned the voltage setting of the mirror electrodes to shift the focus to the point where the best resolution was obtained.

Fig. 9 displays the Δt and R at various laps; Δt is measured by the oscilloscope, and R is calculated by the corresponding time and Δt . As the number of laps increased, Δt (black triangle in Fig. 9) tended to increase rapidly at first and then slowly over hundreds of laps. The primary reason is the time–energy focus condition, which cannot be preserved after every turn. Meanwhile, mass resolution (red circle in Fig. 9) shows a steady upward trend, it is increasing with the lap number, except for a stagnation for the highest lap numbers. To maximize the instrument’s performance, Δt must be controlled.

Fig. 9. Measured Δt and resolution of $^{133}\text{Cs}^+$ ions as a function of the number of laps performed in the MRTOF-MS.

Fig. 10 shows an example of a TOF peak of Cs^+ ions with the fitting function. The TOF peaks were fitted with a Gauss function to obtain the mean TOF and their uncertainties. A mass resolution of up to $R_{\text{FWHM}} = 116,050$ for Cs^+ is achieved after 600 laps of reflection, corresponding to a flight distance of about 1.08 km and a TOF of about 18.02 ms, with an FWHM of 77.65 ns.

Fig. 10. Mass spectrum of $^{133}\text{Cs}^+$ ions for 600 laps measured by API-MRTOF-MS. The red curves are the fitted results with a Gaussian function, demonstrating the mass resolution $R_{\text{FWHM}} = 116,050$. The peak width refers to the FWHM.

CONCLUSION

An API-MRTOF-MS was built and tested with an ESI source. A resolution of $R_{\text{FWHM}} = 116,000$ was achieved with an extremely short measurement time at the millisecond level. The performance demonstrates that the API-MRTOF-MS, with its fast analysis speed and high selectivity, is especially suitable for high-resolution process analysis. This achievement will facilitate the implementation of API-MRTOF-MS in various scientific fields, such as the analysis of transient processes in chemistry, biology, and medicine, and will therefore promote the rapid growth of these disciplines.

ACKNOWLEDGMENTS

We are grateful to the National Natural Science Foundation of China (Grants No. 41827804) and Guangdong Special Support Program (Grants No. 2019BT02Z546) for financial support of this work.

- (1) Wollnik, H.; Casares, A. An energy-isochronous multi-pass time-of-flight mass spectrometer consisting of two coaxial electrostatic mirrors. *International Journal of Mass Spectrometry* **2003**, *227* (2), 217-222.
- (2) Wollnik, H.; Przewloka, M. Time-of-flight mass spectrometers with multiply reflected ion trajectories. *International journal of mass spectrometry and ion processes* **1990**, *96* (3), 267-274.
- (3) Plaß, W. R.; Dickel, T.; Czok, U.; Geissel, H.; Petrick, M.; Reinheimer, K.; Scheidenberger, C.; I.Yavor, M. Isobar separation by time-of-flight mass spectrometry for low-energy radioactive ion beam facilities. *Nuclear Instruments and Methods in Physics Research Section B: Beam Interactions with Materials and Atoms* **2008**, *266* (19), 4560-4564. DOI: <https://doi.org/10.1016/j.nimb.2008.05.079>.
- (4) Piechaczek, A.; Shchepunov, V.; Carter, H. K.; Batchelder, J. C.; Zganjar, E. F.; Liddick, S. N.; Wollnik, H.; Hu, Y.; Griffith, B. O. Development of a high resolution isobar separator for study of exotic decays. *Nuclear Instruments and Methods in Physics Research Section B: Beam Interactions with Materials and Atoms* **2008**, *266* (19), 4510-4514. DOI: <https://doi.org/10.1016/j.nimb.2008.05.149>.
- (5) Schury, P.; Okada, K.; Shchepunov, S.; Sonoda, T.; Takamine, A.; Wada, M.; Wollnik, H.; Yamazaki, Y. Multi-reflection time-of-flight mass spectrograph for short-lived radioactive ions. *European Physical Journal A* **2009**, *42* (3), 343-349, Article. DOI: [10.1140/epja/i2009-10882-6](https://doi.org/10.1140/epja/i2009-10882-6) Scopus.
- (6) Dickel, T.; Jesch, C.; Plaß, W. R.; Ayt, S.; Czok, U.; Geissel, H.; Lautenschläger, F.; Petrick, M.; Scheidenberger, C.; Sun, B.; et al. Further advances in the development of a multiple-reflection time-offlight

mass spectrometer for isobar separation and mass measurements at the LEB. *GSI Sci. Rep.* **2011** , 2010 , Article. Scopus.

(7) Wolf, R.; Beck, D.; Blaum, K.; Böhm, C.; Borgmann, C.; Breitenfeldt, M.; Herfurth, F.; Herlert, A.; Kowalska, M.; Kreim, S. On-line separation of short-lived nuclei by a multi-reflection time-of-flight device. *Nuclear Instruments and Methods in Physics Research Section A: Accelerators, Spectrometers, Detectors and Associated Equipment* **2012** , 686 , 82-90.

(8) Ito, Y.; Schury, P.; Wada, M.; Naimi, S.; Sonoda, T.; Mita, H.; Arai, F.; Takamine, A.; Okada, K.; Ozawa, A. Single-reference high-precision mass measurement with a multireflection time-of-flight mass spectrograph. *Physical Review C* **2013** , 88 (1), 011306.

(9) Weber, C.; Müller, P.; Thierolf, P. G. Developments in Penning trap (mass) spectrometry at MLLTRAP: Towards in-trap decay spectroscopy. *International Journal of Mass Spectrometry* **2013** , 349-350 , 270-276. DOI: <https://doi.org/10.1016/j.ijms.2013.05.006>.

(10) Van Schelt, J.; Lascar, D.; Savard, G.; Clark, J. A.; Bertone, P. F.; Caldwell, S.; Chaudhuri, A.; Levand, A. F.; Li, G.; Morgan, G. E.; et al. First Results from the CARIBU Facility: Mass Measurements on the r -Process Path. *Physical Review Letters* **2013** , 111 (6), 061102. DOI: 10.1103/PhysRevLett.111.061102.

(11) Moore, I. D.; Eronen, T.; Gorelov, D.; Hakala, J.; Jokinen, A.; Kankainen, A.; Kolhinen, V. S.; Koponen, J.; Penttilä, H.; Pohjalainen, I.; et al. Towards commissioning the new IGISOL-4 facility. *Nuclear Instruments and Methods in Physics Research Section B: Beam Interactions with Materials and Atoms* **2013** , 317 , 208-213. DOI: <https://doi.org/10.1016/j.nimb.2013.06.036>.

(12) Yoon, J. W.; Park, Y.-H.; Park, S. J.; Kim, G. D.; Kim, Y. K. Design of the multi-reflection time-of-flight mass spectrometer for the RAON facility. *EPJ Web of Conferences* **2014** , 66 , 11042.

(13) Tian, Y. L.; Wang, Y. S.; Wang, J. Y.; Zhou, X. H.; Huang, W. X. Designing a multi-reflection time-of-flight mass analyzer for LPT. *International Journal of Mass Spectrometry* **2016** , 408 , 28-32. DOI: <https://doi.org/10.1016/j.ijms.2016.08.013>.

(14) Schury, P.; Niwase, T.; Wada, M.; Brionnet, P.; Chen, S.; Hashimoto, T.; Haba, H.; Hirayama, Y.; Hou, D. S.; Iimura, S.; et al. First high-precision direct determination of the atomic mass of a superheavy nuclide. *Physical Review C* **2021** , 104 (2), L021304. DOI: 10.1103/PhysRevC.104.L021304.

(15) Makarov, A.; Denisov, E.; Lange, O. Performance evaluation of a high-field orbitrap mass analyzer. *Journal of the American Society for Mass Spectrometry* **2009** , 20 (8), 1391-1396. DOI: 10.1016/j.jasms.2009.01.005.

(16) Madeira, P. J. A.; Alves, P. A.; Borges, C. M. High resolution mass spectrometry using FTICR and orbitrap instruments. *Fourier Transform–Materials Analysis* **2012** .

(17) San Jose, C., USA and Bremen, Germany Quantitative and Qualitative Confirmation of Pesticides in Beet Extract Using a Hybrid Quadrupole-Orbitrap Mass Spectrometer., *Thermo Scientific Application Note 617* **2015** .

(18) Hondo, T.; Jensen, K. R.; Aoki, J.; Toyoda, M. A new approach for accurate mass assignment on a multi-turn time-of-flight mass spectrometer. *European Journal of Mass Spectrometry* **2017** , 23 (6), 385-392.

(19) Johnson, J. T.; Lee, K. W.; Bhanot, J. S.; McLuckey, S. A. A Miniaturized Fourier Transform Electrostatic Linear Ion Trap Mass Spectrometer: Mass Range and Resolution. *Journal of the American Society for Mass Spectrometry* **2019** , 30 (4), 588-594. DOI: 10.1007/s13361-018-02126-x.

(20) Liu, L.; Li, J.; Lv, J.; Jiang, H.; Chen, F.-e. Detoxification mechanism of vinegar-processed Kansui revealed by systematic phytochemical analysis using ultrahigh-performance liquid chromatography diode array detection tandem mass spectrometry, ultrahigh-performance liquid chromatography high-resolution

mass spectrometry and in silico drug target identification. *Rapid Communications in Mass Spectrometry* **2022** , *36* (17), e9332. DOI: <https://doi.org/10.1002/rcm.9332>.

(21) Kotiaho, T. On-site environmental and in situ process analysis by mass spectrometry. *Journal of Mass Spectrometry* **1996** , *31* (1), 1-15.

(22) Kueppers, S.; Haider, M. Process analytical chemistry—future trends in industry. *Analytical and Bioanalytical Chemistry* **2003** , *376* (3), 313-315. DOI: [10.1007/s00216-003-1907-0](https://doi.org/10.1007/s00216-003-1907-0).

(23) Hinz, D. C. Process analytical technologies in the pharmaceutical industry: the FDA's PAT initiative. *Analytical and Bioanalytical Chemistry* **2006** , *384*(5), 1036-1042. DOI: [10.1007/s00216-005-3394-y](https://doi.org/10.1007/s00216-005-3394-y).

(24) Holmes, N.; Akien, G. R.; Savage, R. J. D.; Stanetty, C.; Baxendale, I. R.; Blacker, A. J.; Taylor, B. A.; Woodward, R. L.; Meadows, R. E.; Bourne, R. A. Online quantitative mass spectrometry for the rapid adaptive optimisation of automated flow reactors. *Reaction Chemistry & Engineering* **2016** , *1* (1), 96-100, [10.1039/C5RE00083A](https://doi.org/10.1039/C5RE00083A). DOI: [10.1039/C5RE00083A](https://doi.org/10.1039/C5RE00083A).

(25) Zhang, J.; Li, Z.; Zhou, Z.; Bai, Y.; Liu, H. Rapid screening and quantification of glucocorticoids in essential oils using direct analysis in real time mass spectrometry. *Rapid Communications in Mass Spectrometry* **2016** , *30* (S1), 133-140. DOI: <https://doi.org/10.1002/rcm.7639>.

(26) Transient Processes. In *Chemical Engineering Design and Analysis: An Introduction* , Reimer, J. A., Duncan, T. M. Eds.; Cambridge Series in Chemical Engineering, Cambridge University Press, 1998; pp 310-350.

(27) Huang, M.-Z.; Cheng, S.-C.; Cho, Y.-T.; Shiea, J. Ambient ionization mass spectrometry: A tutorial. *Analytica Chimica Acta* **2011** , *702* (1), 1-15. DOI: <https://doi.org/10.1016/j.aca.2011.06.017>.

(28) Liu, Q.; Zenobi, R. Rapid analysis of fragrance allergens by dielectric barrier discharge ionization mass spectrometry. *Rapid Communications in Mass Spectrometry* **2021** , *35* (6), e9021. DOI: <https://doi.org/10.1002/rcm.9021>.

(29) Gao, Y.; Wang, W.; Zhang, K.; Li, Y.; Cai, G. A study on the ionization mechanisms in a miniaturized cylindrical Hall thruster. *Vacuum* **2022** , *201* , 111060. DOI: <https://doi.org/10.1016/j.vacuum.2022.111060>.

(30) Dickel, T.; Plass, W. R.; Lang, J.; Ebert, J.; Geissel, H.; Haettner, E.; Jesch, C.; Lippert, W.; Petrick, M.; Scheidenberger, C.; et al. Multiple-reflection time-of-flight mass spectrometry for in situ applications. *Nuclear Instruments and Methods in Physics Research Section B: Beam Interactions with Materials and Atoms* **2013** , *317* , 779-784. DOI: <https://doi.org/10.1016/j.nimb.2013.08.021>.

(31) Dickel, T.; Plass, W. R.; Lippert, W.; Lang, J.; Yavor, M. I.; Geissel, H.; Scheidenberger, C. Isobar Separation in a Multiple-Reflection Time-of-Flight Mass Spectrometer by Mass-Selective Re-Trapping. *Journal of the American Society for Mass Spectrometry* **2017** , *28* (6), 1079-1090. DOI: [10.1007/s13361-017-1617-z](https://doi.org/10.1007/s13361-017-1617-z).

(32) Naimi, S.; Nakamura, S.; Ito, Y.; Mita, H.; Okada, K.; Ozawa, A.; Schury, P.; Sonoda, T.; Takamine, A.; Wada, M. An rf-carpet electrospray ion source to provide isobaric mass calibrants for trans-uranium elements. *International Journal of Mass Spectrometry* **2013** , *337* , 24-28.

(33) Ring, S.; Pedersen, H.; Heber, O.; Rappaport, M.; Witte, P.; Bhushan, K.; Altstein, N.; Rudich, Y.; Sagi, I.; Zajfman, D. Fourier transform time-of-flight mass spectrometry in an electrostatic ion beam trap. *Analytical chemistry* **2000** , *72* (17), 4041-4046.

(34) Strasser, D.; Heber, O.; Goldberg, S.; Zajfman, D. Self-bunching induced by negative effective mass instability in an electrostatic ion beam trap. *Journal of Physics B: Atomic, Molecular and Optical Physics* **2003** , *36* (5), 953.

(35) Hilger, R. T.; Santini, R. E.; McLuckey, S. A. Nondestructive Tandem Mass Spectrometry Using a Linear Quadrupole Ion Trap Coupled to a Linear Electrostatic Ion Trap. *Analytical Chemistry* **2013** , *85* (10), 5226-5232. DOI: [10.1021/ac4007182](https://doi.org/10.1021/ac4007182).

- (36) Hilger, R. T.; Dziekonski, E. T.; Santini, R. E.; McLuckey, S. A. Injecting electrospray ions into a Fourier transform electrostatic linear ion trap. *International Journal of Mass Spectrometry* **2015** , *378* , 281-287. DOI: <https://doi.org/10.1016/j.ijms.2014.09.005>.
- (37) Verentchikov, A. N.; Yavor, M. I.; Hasin, Y. I.; Gavrik, M. A. Multireflection planar time-of-flight mass analyzer. II: The high-resolution mode. *Technical Physics* **2005** , *50* (1), 82-86. DOI: 10.1134/1.1854828.
- (38) Verenchikov, A.; Kirillov, S.; Khasin, Y.; Makarov, V.; Yavor, M.; Artaev, V. Multiplexing in Multi-Reflecting TOF MS. *Journal of Applied Solution Chemistry and Modeling* **2017** , *6* , 1-22. DOI: 10.6000/1929-5030.2017.06.01.1.
- (39) Cooper-Shepherd, D. A.; Wildgoose, J.; Kozlov, B.; Johnson, W. J.; Tyldesley-Worster, R.; Palmer, M. E.; Hoyes, J. B.; McCullagh, M.; Jones, E.; Tonge, R.; et al. Novel Hybrid Quadrupole-Multireflecting Time-of-Flight Mass Spectrometry System. *Journal of the American Society for Mass Spectrometry* **2023** . DOI: 10.1021/jasms.2c00281.
- (40) Stewart, H.; Grinfeld, D.; Giannakopoulos, A.; Petzoldt, J.; Shanley, T.; Garland, M.; Denisov, E.; Peterson, A.; Damoc, E.; Zeller, M.; et al. Parallelized Acquisition of Orbitrap and Astral Analyzers Enables High-Throughput Quantitative Analysis. *bioRxiv* **2023** , 2023.2006.2002.543408. DOI: 10.1101/2023.06.02.543408.
- (41) Rosenbusch, M.; Wada, M.; Schury, P.; Ito, Y.; Ishiyama, H.; Ishizawa, S.; Hirayama, Y.; Kimura, S.; Kojima, T.; Miyatake, H. A new multi-reflection time-of-flight mass spectrograph for the SLOWRI facility. *Nuclear Instruments and Methods in Physics Research Section B: Beam Interactions with Materials and Atoms* **2020** , *463* , 184-188.
- (42) Rosenbusch, M.; Wada, M.; Chen, S.; Takamine, A.; Iimura, S.; Hou, D.; Xian, W.; Yan, S.; Schury, P.; Hirayama, Y.; et al. The new MRTOF mass spectrograph following the ZeroDegree spectrometer at RIKEN's RIBF facility. *Nuclear Instruments and Methods in Physics Research Section A: Accelerators, Spectrometers, Detectors and Associated Equipment* **2023** , *1047* , 167824. DOI: <https://doi.org/10.1016/j.nima.2022.167824>.
- (43) Wada, M.; Ishida, Y.; Nakamura, T.; Yamazaki, Y.; Kambara, T.; Ohyama, H.; Kanai, Y.; Kojima, T. M.; Nakai, Y.; Ohshima, N. Slow RI-beams from projectile fragment separators. *Nuclear Instruments and Methods in Physics Research Section B: Beam Interactions with Materials and Atoms* **2003** , *204* , 570-581.
- (44) Dodonov, A.; Kozlovski, V.; Soulimenkov, I.; Raznikov, V.; Loboda, A.; Zhen, Z.; Horwath, T.; Wollnik, H. High-resolution electrospray ionization orthogonal-injection time-of-flight mass spectrometer. *European Journal of Mass Spectrometry* **2000** , *6* (6), 481-490.
- (45) Guo, C.; Huang, Z.; Gao, W.; Nian, H.; Chen, H.; Dong, J.; Shen, G.; Fu, J.; Zhou, Z. A homemade high-resolution orthogonal-injection time-of-flight mass spectrometer with a heated capillary inlet. *Review of Scientific Instruments* **2008** , *79* (1), 013109. DOI: 10.1063/1.2832334.
- (46) Javahery, G.; Thomson, B. A segmented radiofrequency-only quadrupole collision cell for measurements of ion collision cross section on a triple quadrupole mass spectrometer. *Journal of the American Society for Mass Spectrometry* **1997** , *8* (7), 697-702.
- (47) Guo, C.; Huang, Z.; Gao, W.; Nian, H.; Chen, H.; Fu, J.; Zhou, Z. Combining a capillary with a radio-frequency-only quadrupole as an interface for a home-made time-of-flight mass spectrometer. *European Journal of Mass Spectrometry* **2007** , *13* (4), 249-257.
- (48) Dawson, P. Performance characteristics of an RF-only quadrupole. *International journal of mass spectrometry and ion processes* **1985** , *67* (3), 267-276.
- (49) Shu-xiong, Y.; Hui, Z.; Ting, M.; Wei, G.; Zheng-xu, H. Application of Ion Valve Technology in an Orthogonal-Injection TOF Mass Spectrometer. *Journal of Chinese Mass Spectrometry Society* **2017** , *38* (3), 294.

- (50) Schury, P.; Okada, K.; Shchepunov, S.; Sonoda, T.; Takamine, A.; Wada, M.; Wollnik, H.; Yamazaki, Y. Multi-reflection time-of-flight mass spectrograph for short-lived radioactive ions. *The European Physical Journal A* **2009** , 42 (3), 343-349. DOI: 10.1140/epja/i2009-10882-6.
- (51) Plass, W. R.; Dickel, T.; Scheidenberger, C. Multiple-reflection time-of-flight mass spectrometry. *International Journal of Mass Spectrometry* **2013** , 349-350 , 134-144. DOI: <https://doi.org/10.1016/j.ijms.2013.06.005>.
- (52) Schury, P.; Wada, M.; Ito, Y.; Arai, F.; Naimi, S.; Sonoda, T.; Wollnik, H.; Shchepunov, V. A.; Smorra, C.; Yuan, C. A high-resolution multi-reflection time-of-flight mass spectrograph for precision mass measurements at RIKEN/SLOWRI. *Nuclear Instruments and Methods in Physics Research Section B: Beam Interactions with Materials and Atoms* **2014** , 335 , 39-53. DOI: <https://doi.org/10.1016/j.nimb.2014.05.016>.
- (53) Pfeiffer Vacuum, G. Vacuum technology book. *Vol. II, Pfeiffer Vacuum GmbH, Asslar, Germany* **2013** .
- (54) Reynolds, O. XXIX. An experimental investigation of the circumstances which determine whether the motion of water shall be direct or sinuous, and of the law of resistance in parallel channels. *Philosophical Transactions of the Royal society of London* **1883** , (174), 935-982.
- (55) Urban, J.; Štys, D. Noise and baseline filtration in mass spectrometry. In *Bioinformatics and Biomedical Engineering: Third International Conference, IWBBIO 2015, Granada, Spain, April 15-17, 2015. Proceedings, Part II 3* , 2015; Springer International Publishing: pp 418-425.